# Force and Velocity Measured for Single Molecules of RNA Polymerase

**Michelle D. Wang,\* Mark J. Schnitzer, Hong Yin,†
Robert Landick, Jeff Gelles, Steven M. Block‡**

RNA polymerase (RNAP) moves along DNA while carrying out transcription, acting as a molecular motor. Transcriptional velocities for single molecules of *Escherichia coli* RNAP were measured as progressively larger forces were applied by a feedback-controlled optical trap. The shapes of RNAP force-velocity curves are distinct from those of the motor enzymes myosin or kinesin, and indicate that biochemical steps limiting transcription rates at low loads do not generate movement. Modeling the data suggests that high loads may halt RNAP by promoting a structural change which moves all or part of the enzyme backwards through a comparatively large distance, corresponding to 5 to 10 base pairs. This contrasts with previous models that assumed force acts directly upon a single-base translocation step.

RNA polymerase (RNAP) carries out an essential step of gene expression, the synthesis of an RNA copy of the template DNA. Each RNA molecule is synthesized in its entirety by a single molecule of RNAP moving processively along the template. Movement is powered by the free energy liberated as appropriate nucleoside triphosphates (NTPs) are joined to the 3′-end of the nascent RNA chain, pyrophosphate ($PP_i$) is released, and the growing transcript folds (*1*). During transcript elongation, *Escherichia coli* RNAP progresses along DNA at speeds >10 nucleotides per second (at 25°C), and generates considerable force (>14 pN) (*2*). RNAP is thus a true motor protein, akin to cytoskeletal motors of the myosin, kinesin, or dynein families. Enzyme movement has been characterized in vitro using light or scanning-force microscopy techniques capable of detecting movement by single molecules (*2–4*), and transcription complexes have been manipulated using forces supplied by an optical trap (*2*). By determining the micromechanical properties of RNAP and correlating this information with results from biochemical kinetic studies, we hope to shed light on the mechanism of transcript elongation.

M. D. Wang and S. M. Block, Department of Molecular Biology and Princeton Materials Institute, Princeton University, Princeton, NJ 08544, USA. M. J. Schnitzer, Departments of Physics and Molecular Biology, Princeton University, Princeton, NJ 08544, USA. H. Yin and J. Gelles, Department of Biochemistry, Brandeis University, Waltham, MA 02254, USA. R. Landick, Department of Bacteriology, University of Wisconsin, Madison, WI 53706, USA.

\*Present address: Department of Physics, Cornell University, Ithaca, NY 14853, USA.
†Present address: Department of Physiology, Tufts University Medical School, Boston, MA 02111, USA.
‡To whom correspondence should be addressed. E-mail: block@princeton.edu

A central unresolved feature in the RNAP mechanism is the nature of the reaction steps that lead to movement (*1, 5*). Such steps can be characterized by applying mechanical loads opposing forward motion: provided that the external forces are not so large as to disrupt enzyme structure, this manipulation will tend to perturb selectively the rates of translocation steps. The relationship between applied force *F* and steady-state velocity *V* is therefore a fundamental characteristic of the enzyme mechanism itself. *F-V* relationships have been determined for three biological motors: ensembles of myosin in contracting muscles (*6*), single molecules of kinesin moving along microtubules (*7*), and the rotary engine that spins bacterial flagella (*8*). Here, we report high-resolution measurements of the *F-V* relationship for *E. coli* RNAP. The shapes of the *F-V* curves imply that translocation steps do not limit transcription rates when loads are low. Moreover, the curves are consistent with a class of models where translocation steps entail motions through unexpectedly large distances along the template (corresponding to 5 to 10 base pairs), either in the form of conformational changes taking place within the enzyme itself or as translational motions of the enzyme complex with respect to the DNA.

## Experimental Design

The experimental geometry of our previous study (*2*) employed a fixed optical trap to exert a variable force on a microscopic bead attached to the downstream end of a DNA template [Fig. 1A; see also figure 1 of (*2*)]. As a bead is pulled from the trap center (by RNAP fixed to a coverglass surface and actively transcribing at the opposite end of the DNA tether), an optical restoring force builds up until it just balances the force exerted by

RNAP, at which point transcriptional progress stops, often reversibly. This arrangement is conducive to static measurements of the stall force, once motion has ceased, but is less well-suited to making dynamic measurements of force and velocity, because DNA stretches under changing loads and elasticity varies as the tether length changes during the experiment. The series compliance of the elastic linkage must be taken into account to derive the displacement of the RNAP with respect to the DNA from records of bead position. To meet this challenge, we developed a feedback-controlled instrument that optically clamps the position of a bead in the trap and facilitates rapid, accurate measurements of force (*9*).

Figure 1, A through C, demonstrates the performance of the instrument in its open-loop mode (feedback inactive), recording the displacement of a bead held in a weak trap of fixed stiffness and subjected to variable force (*10*). Transcriptional elongation rates were comparable to those reported earlier (generally, ~2 to 5 nm/s) (*3*). In closed-loop mode (Fig. 1, D through F), elongation proceeds at low trap stiffness until the clamp limit is reached and the feedback circuit is triggered. Thereafter, the bead position is actively maintained as the trap stiffness, which is proportional to force at this position, rises to compensate. Two representative stalls are shown (*11*). After the first stall was completed and the clamp released, the elasticity stored in the DNA tether abruptly pulled the bead forward by an additional ~50 nm. Force was then reduced by moving the optical trap position (at *t* = 46 s), but transcription did not resume for another ~30 s, indicating that the transcription complex had entered into some kind of inactive state (discussed below). A second stall was produced after transcriptional activity resumed, and the feedback was enabled once the bead had been allowed to travel ~25 nm beyond the clamp limit. The abrupt response at this point illustrates the elasticity of the tether. In either case, transcription stalled at a trap stiffness of 0.25 to 0.29 pN/nm, corresponding to a force of 30 to 35 pN (*12*).

## Force and Velocity Measurements

Once trap properties are calibrated and adjustments are made for series compliance, it is possible to convert measurements of bead displacement and trap stiffness directly into records of time-varying force and RNAP position along the template, and thereby into RNA transcript length (*13*). Figure 2 shows such scaling for motion in both low-load ($0 < F < 5$ pN, open-loop; Fig. 2, A and B) and high-load ($5 < F < 50$ pN, closed-loop; Fig. 2, C and D) regimes. In general, RNAP moved under low loads at an average velocity of 16 nucleotides per second (for 1 mM

NTPs; 1 μM PP$_i$) or 7 nucleotides per second (for 1 mM NTPs; 1 mM PP$_i$). All single-molecule records displayed periods of steady transcriptional elongation interrupted by pauses, during which tension was maintained but elongation ceased, lasting from ~1 to 10 s (arrows; Fig. 2, B and D). Transcriptional pauses of comparable durations are also detected at negligible loads in conventional biochemical studies of transcription in solution (14). After algorithmic deletion of pauses, records showed the elongation rate to be remarkably constant (15), up to external loads nearly sufficient to stall the complex (Fig. 2, C and D).

The distribution of stall forces is obtained from the maximum loads supported with the position clamp active (Fig. 3, A and B). In the presence of saturating NTPs and 1 μM PP$_i$, the stall force was ~25 pN. Raising the PP$_i$ concentration to 1 mM slowed the mean elongation rate at low force by 2.3-fold and yielded a stall force of ~23 pN, which is not significantly different. This change reduces the estimated free energy $\Delta G$ for the RNAP condensation reaction by mass action from –7.2 to –3.1 kcal/mol (2). Assuming that every reaction cycle carries RNAP forward on average by a single base unit, the fraction of free energy converted into mechanical work near stall is estimated at ~44% (at 1 mM PP$_i$ or ~18% at 1 μM PP$_i$) (16). In this respect, RNAP resembles kinesin, which expends roughly half its available free energy as mechanical work near stall (17).

From adjusted records of force and velocity as functions of time (Fig. 2, C and D), we derive single-molecule F-V curves, an example of which is shown (Fig. 4A). Remarkably, the shapes of these curves were highly convex, in contrast to muscle, which follows a concave (hyperbolic) F-V relationship (6), or kinesin, which is fairly linear (7). Velocity remained nearly independent of load out to a significant force, approaching stall (18). Pausing introduces characteristic notches in F-V curves, as the velocity transiently drops to zero with no change in the applied load. Pause-induced notches do not reflect the elongation process per se, but a secondary process presumably correlated with sequence. Thus, pauses complicate the analysis of force-velocity data. We took two approaches to deal with these: (i) we averaged them out, combining F-V data from individual complexes (a procedure that succeeds only if pauses are infrequent and occur at random), or (ii) we artificially removed them from individual records, by means of an algorithm that deletes segments during which the average velocity dropped below some predefined threshold. Both methods produced similar results. The large heterogeneity of forces produced by RNAP (Fig. 3) and considerable variation in elongation rates at low

loads (3, 19) further complicate analysis.

To combine multiple single-molecule F-V curves, we first parameterized these in terms of v, a dimensionless velocity (normalized to the unloaded speed $V_0$), and f, a dimensionless force (normalized to the force at half-maximal velocity $F_{1/2}$), before averaging. This procedure is justified in light of a large class of tightly coupled enzymatic mechanisms for elongation, all of which lead to the simple functional form $v(f) = 1/(1 + a^{f-1})$, which depends only on a single free parameter, a (see Appendix). Averaged f-v curves were determined for two concentrations of PP$_i$ (Fig. 4, B and C). From the fitted values of x and $\langle F_{1/2} \rangle$, a "characteristic distance" δ over which load acts can be computed, ac-

cording to $\delta = k_B T \ln(a)/\langle F_{1/2} \rangle$ (Appendix, Eq. 9). Experimental estimates for δ are inevitably subject to error, primarily through their logarithmic dependence on a. Here, δ ranged from ~5 to 10 base pairs (Fig. 4). The physical interpretation of this distance depends on the biochemical model invoked.

## Comparisons with Theory

The model we favor, which draws support from recent biochemical work, interprets a mechanical stall as an elongation-incompetent state branching off the main reaction pathway (Appendix, Eq. 6), reached in a load-dependent manner (20). One specific instance of an elongation-incompetent state, among several known to exist (21), would be
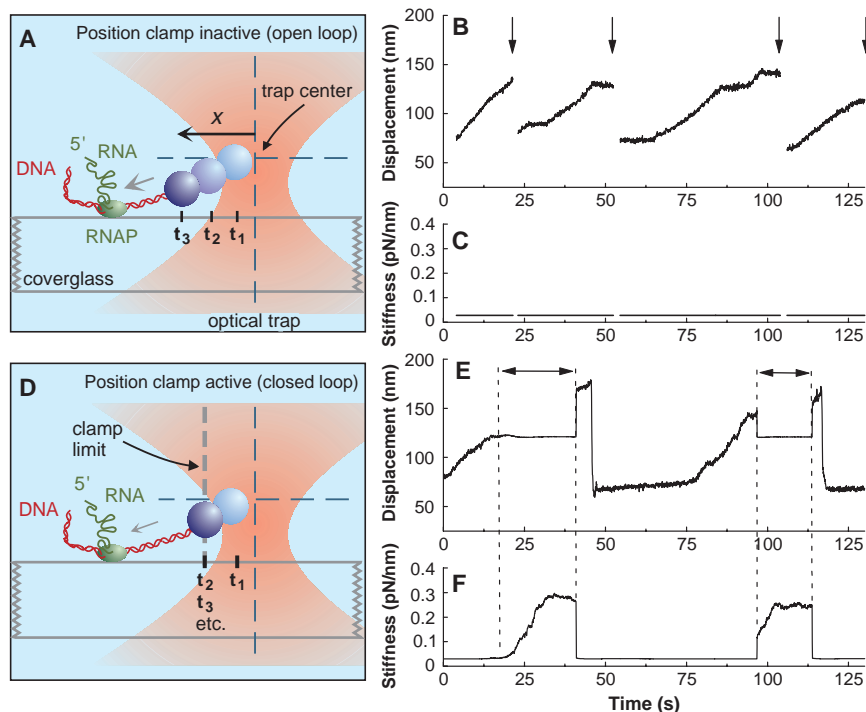


**Fig. 1.** Comparison of open- and closed-loop trapping modes to observe translocation by RNAP. (**A**) Cartoon illustrating the experimental geometry with the position clamp inactive (not to scale). A ternary complex consisting of RNAP (green ellipsoid), the DNA template (red), and a nascent RNA chain (green) is fixed to a coverglass surface inside a flow cell. A polystyrene bead (blue sphere), attached to the transcriptionally-downstream end of the DNA, is captured and held under low tension by the optical trap (pink gradient). Subsequent displacement of the bead, x (arrow), is detected interferometrically. As transcription proceeds, DNA is drawn through the polymerase, pulling the bead from the trap center (intersection of dashed blue lines) at successive times $t_1$, $t_2$, $t_3$, and so forth. (**B**) Displacement versus time for low loads. Once the bead moved through the usable range of the interferometer (~150 nm), the trap was manually repositioned closer to the polymerase, at the times indicated (arrows). Note the variability in speed caused by transcriptional pausing. In this experiment, applied force at the maximum displacement was ~4 pN, well below the RNAP stall force. (**C**) Corresponding trap stiffness (0.03 pN/nm, invariant in this mode). (**D**) Position clamp active. Initial configuration is identical to (A). During the interval $t_1$–$t_2$, RNAP draws the bead from the trap until the clamp limit is reached (gray dashed line) and activates the feedback circuit. Thereafter (at $t_2$, $t_3$, . . .) laser intensity is servo-controlled to prevent displacement. (**E**) Displacement versus time. The clamp limit was set to 121 nm and activated during the intervals indicated (arrows). For the first stall, the clamp was triggered automatically when the limit was reached ($t = 16$ s) and maintained until after stall. Upon release, the bead position jumped because of stored elastic energy in the tether ($t = 40$ s). The trap was manually repositioned for a second run ($t = 46$ s). Here, the bead was allowed to proceed somewhat beyond the limit, and the clamp was triggered manually ($t = 97$ s). (**F**) Corresponding change in stiffness. During the first stall, stiffness rose from 0.03 to 0.29 pN/nm (35 pN). During the second stall, stiffness rose from 0.03 to 0.25 pN/nm (30 pN). Experimental conditions: 1 mM NTP (each), 1 μM PP$_i$.

for RNAP to stop RNA synthesis and slide backward a short distance along the template (5 to 10 base pairs, or ~2 to 3 nm), yet maintain register between RNA and DNA. Subsequently, upon reduction of load, the enzyme would slide forward by the identical distance and resume transcription at the next template site. This sequence corresponds precisely to what has been proposed for one type of transcriptional pause and subsequently observed in at least one case (22, 23): the scenario is roughly analogous to backing up, then advancing, a stuck zipper. If this interpretation holds, then the application of an external load causes RNAP to enter a biochemical state similar to—perhaps identical with—a transcriptional pause. Consistent with this, not all complexes stalled by the force clamp started up immediately upon reduction of load; in a significant fraction of cases, motion began after a variable lag, ranging from 0 to 30 s (Fig. 1F), a time comparable to the lifetimes of certain transcriptional pauses. An alternative possibility is that RNAP moves bidirectionally on the template through a distance corresponding to δ before committing to a load-dependent translocation step, which results in the addition of one nucleotide to the nascent RNA chain (Appendix, Eq. 5). Although these models differ in significant details, they have three essential features in common. First, their reaction schemes are tightly coupled; the enzyme carries out one condensation reaction per base pair moved along the DNA. Second, they

involve large-scale movements of the enzyme associated with mechanical stalling; the sharp drop in velocity as force approaches stall is incompatible with a load-dependent step with δ ≈ 1 base pair. Thus, the data are inconsistent with a simple model wherein force acts only by blocking a step that moves the enzyme by a single base pair. Third, the convex shapes of *F-V* curves arise because the rate-limiting biochemical transition is not load-dependent over most of the force range (24).

Two theoretical treatments of RNAP elongation have recently been published which manifest these very same general features (25, 26) and also generate convex *F-V* relationships, in agreement with preliminary data from our work (27). In one, conformational changes taking place within a flexible RNAP molecule cause it to alternate between stressed and relaxed states, deforming by a variable distance corresponding to 0 to 8 base pairs (26). In the other, the 3′-end of the RNA undergoes thermal fluctuations against a physical barrier represented by the enzyme catalytic site; rectification of this random motion, driven by the free energy of nucleotide condensation, produces a "Brownian ratchet" that can exert significant force (25). In such models, the enzymatic turnover remains relatively independent of increases in force until the load-dependent transition slows to the point where it requires a time comparable to one or more other rates (25). Beyond this force, speed drops precipitously. Although their microscopic mechanisms are distinct, in

certain limiting cases both treatments become equivalent to the class of mechanisms considered in the Appendix.

Determining whether RNAP moves by a Brownian ratchet, conformational change, or some other means and elucidating the reaction pathway of the mechanism will require detailed knowledge not only of the biochemical steps catalyzed by the enzyme, but also of its mechanical states. Of particular interest will be sequence-specific aspects of RNAP behavior (transcriptional pausing, stalling, and arrest), as well as the response of the transcription complex to cofactors involved in initiation, termination, antitermination, and so forth. We anticipate that single-molecule experiments will continue to supply new insights into the behavior of this fascinating enzyme.

### Appendix: One-Parameter *F-V* Analysis

Several classes of mechanochemical models lead to *F-V* relations of the general Boltzmann form

$$V(F) = \frac{V_0(1 + A)}{1 + A\exp(F\delta/k_B T)} \quad (1)$$

where $V_0$ is the velocity at zero load, δ is a characteristic distance, and $A$ is a dimensionless constant that determines the degree to which either mechanical or biochemical events limit the enzymatic cycle at vanishing load: biochemical transitions are rate-limiting for $A \ll 1$, whereas mechanical transitions become limiting when $A \gtrsim 1$. The simplest class of models yielding Eq. 1 involves a sequence of reversible reactions between $N$
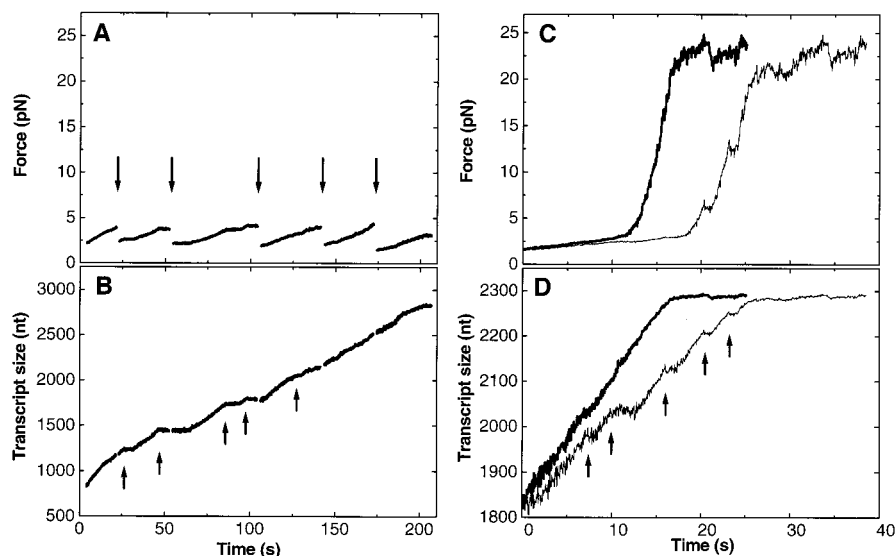


**Fig. 2.** Transcription at low and high loads. (**A**) Force produced by RNAP and (**B**) the corresponding length of the RNA transcript versus time at low load (open-loop mode). Transcript size was computed from the corrected displacements of beads, as described. The trap was repositioned manually at the times indicated [arrows (A)] to maintain the bead within detection range; displacement records were concatenated at these points. Transcriptional pauses of varying duration occur [arrows (B)]. (**C**) Force and (**D**) corresponding transcript length at high load (closed-loop mode). Force increased until the complex stalled at ~23 pN. Original traces (thin lines) contain transcriptional pauses [arrows (D)], which were deleted by an editing algorithm (thick lines) (15). Experimental conditions: 1 mM NTP, 1 μM PP$_i$.
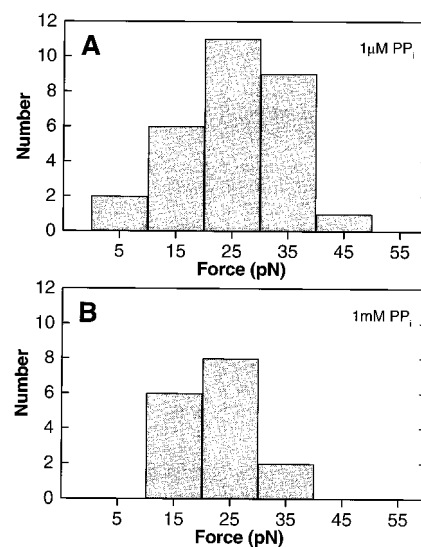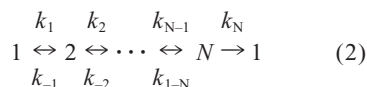


**Fig. 3.** Histograms of RNAP stall force. (**A**) Stall force distribution for 1 mM NTP, 1 μM PP$_i$. Average force was 25.0 ± 1.7 pN (mean ± SEM; $n$ = 29). (**B**) Stall force distribution for 1 mM NTP, 1 mM PP$_i$. Average force was 22.9 ± 1.9 pN ($n$ = 16). The difference in values is not significant ($t$ test, $P$ = 0.44).

intermediate states, followed by a single irreversible reaction, a mechanical transition that carries polymerase from one site to the next

$$
\begin{array}{ccccc}
k_1 & k_2 & & k_{N-1} & k_N \\
1 \leftrightarrow & 2 \leftrightarrow & \cdots & \leftrightarrow N & \rightarrow 1 \\
k_{-1} & k_{-2} & & k_{1-N} &
\end{array} \qquad (2)
$$

In this scheme, the translocation rate $k_N$ is governed by Arrhenius/Eyring kinetics; hence, it depends exponentially on the height of the energy barrier between the two sites (Fig. 5). The application of an external load, $F$, raises the barrier by $F\Delta$ and slows the rate according to

$$
k_N = k_N^0 \exp(-F\Delta/k_B T) \qquad (3)
$$

From the differential equations describing the pathway in Eq. 2, it can be shown that the overall time to complete an enzymatic cycle, $\tau$, is a sum of two times, one which is independent of force and the other which increases exponentially with force

$$
\tau = \tau_1 + \tau_2 \exp(F\Delta/k_B T) \qquad (4)
$$

The reciprocal of Eq. 4 leads directly to an expression for velocity that is equivalent to Eq. 1. For this class of models, the distance $\delta$ in Eq. 1 corresponds to $\Delta$, the distance from the initial site to the position of the barrier maximum (Fig. 5).
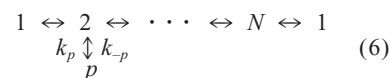
A second class of models also takes the form of the reaction pathway in Eq. 2. However, in this class, one among the states 1 to $N$ is actually a load-dependent composite of two sequential substates that are in rapid equilibrium and located at adjacent physical sites along the DNA (28). (In fact, the earlier requirement for an irreversible reaction leading from state $N$ may now be relaxed somewhat. The condition $\bar{k}_{-i}/\bar{k}_i \ll \exp(-Fd/Nk_B T)$, where the bars denote a geometric mean over the $N$ states, suffices.) For a transition from the composite state to proceed, the enzyme must occupy the forward-most of the two sites. Thus, the rate of enzyme progress is proportional to the relative occupancy of the forward and rearward sites, $p_+/p_-$, which varies exponentially with their relative energies as

$$
\frac{p_+}{p_-} = K \exp(-Fd/k_B T) \qquad (5)
$$

The constant $K$ determines the zero-load equilibrium between forward and rearward substates. As before, it can be shown that the average time to complete a cycle is a sum of terms independent of load and exponentially dependent upon load, once again leading to the same functional form as Eq. 1. However, for this particular class of models, $\delta$ is now identified with $d$, the physical distance between the forward and rearward sites on the DNA (Fig.

5). (In neither this scheme nor in the previous one is $\delta$ restricted to represent the distance subtended by a single base pair; integral multiples of this distance are permitted.)

A third class of models leading to Eq. 1 involves fully reversible reactions, plus an elongation-incompetent ("halted") state $p$ branching off the main pathway, the transition to which is load-dependent

$$
\begin{array}{ccccc}
1 & \leftrightarrow & 2 & \leftrightarrow \cdots \leftrightarrow N \leftrightarrow 1 \\
 & & k_p \updownarrow k_{-p} & \\
 & & p &
\end{array} \qquad (6)
$$

The pathway of Eq. 6 shows state $p$ arising directly from state 2, but the location of this branch point is arbitrary and causes no loss of generality, because state labels are arbitrary and may be permuted. The force dependence in Eq. 6 arises because the rate to enter the halted state $k_p$ and the rate to return to the main pathway $k_{-p}$ both obey Arrhenius behavior

$$
k_p = k_p^0 \exp(F\Delta/k_B T)
$$

and

$$
k_{-p} = k_{-p}^0 \exp[-F(d - \Delta)/k_B T] \qquad (7)
$$

The average number of visits to state $p$ rises linearly with $k_p$, and the average time delay per visit is $1/k_{-p}$. The total delay that the enzyme experiences because of the halted state is proportional to $k_p/k_{-p}$ and thus to $\exp(Fd/k_B T)$. This exponentially dependent delay, when combined with other biochemical waiting times that are independent of force, again leads to Eq. 1, with $\delta = d$. For this class of models, the distance $d$ characterizes the physical extent of the conformational change between the competent and incompetent states and need not correspond to an integral multiple of base pairs.

Equation 1 may be used to derive a useful scaling formula, permitting data from individual RNAP molecules manifesting differ-

**Fig. 4.** Individual molecule and averaged force-velocity relationships for RNAP. (**A**) Example of a single-molecule *F-V* curve, derived from the data of Fig. 2, C and D. Notches produced by transcriptional pausing appear in unprocessed data (dotted line), but are absent in data from edited traces (solid line). Experimental conditions: 1 mM NTP, 1 μM PPi. (B and C) Averaged *F-V* curves. Individual curves were normalized as described. (**B**) Ensemble average for eight complexes in 1 mM NTP, 1 mM PP$_i$; showing data with (thin solid line) and without (thin dotted line) pauses removed. Fit to the *f*-*v* relationship (Appendix, Eq. 11, thick lines). Fit parameter $a = 5.08 \pm 4.11 \times 10^4$; $\langle F_{1/2} \rangle = 15.8$ pN, corresponding to $\delta$ in the range 4.6 to 5.2 bp. (**C**) Ensemble average for 13 complexes in 1 mM NTP, 1 μM PP$_i$. Fit parameter $a = 1.96 \pm 0.99 \times 10^4$; $\langle F_{1/2} \rangle = 23.9$ pN, corresponding to $\delta$ in the range 7.0 to 8.7 bp.
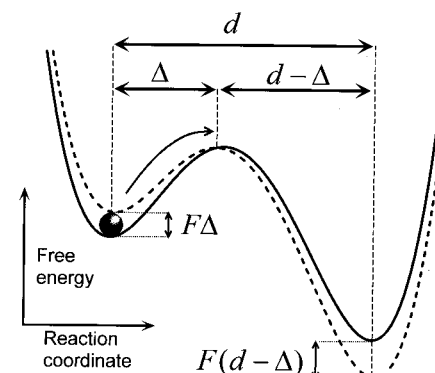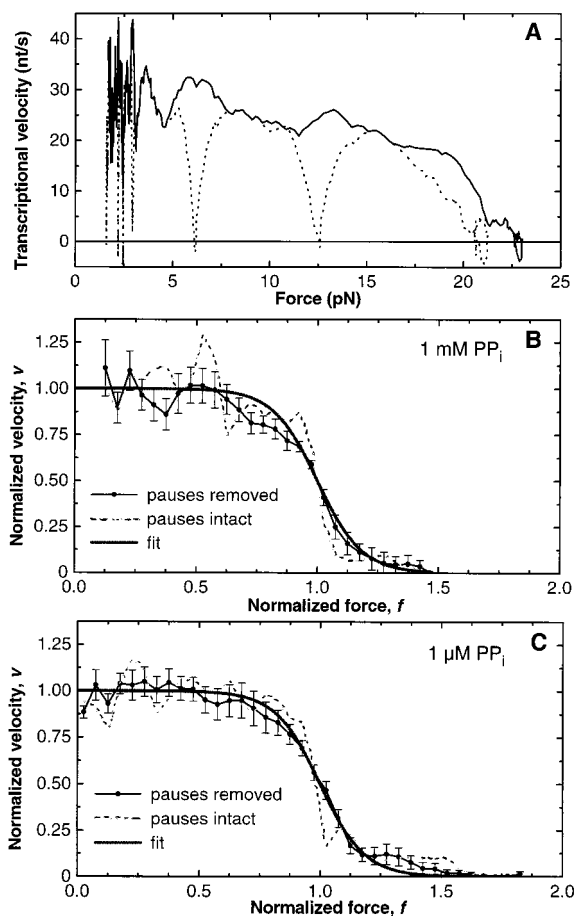


**Fig. 5.** Schematic energy diagram, depicting a single barrier between two potential wells separated by distance $d$. The barrier is a distance $\Delta$ from the initial site, where RNAP (sphere) begins its cycle. The application of an external load, $F$, alters the potential by the amounts indicated (dotted line, initial; solid line, final).

ent speeds or forces, or both, to be normalized and therefore compared. For example, the random orientation of molecules on the surface with respect to the direction of the applied load in this assay may represent one cause of heterogeneity in stall force (29). Alternatively, individual molecules might display different unloaded rates, $V_0$, but nevertheless, the relative biochemical and mechanical contributions to the kinetics (identified with constant $A$) might remain the same. Moreover, small differences in $\delta$ are exponentially magnified, generating significant differences in stall forces between otherwise similar complexes. To normalize away heterogeneity, we divide Eq. 1 by the maximum velocity, yielding a dimensionless velocity, $v$

$$v = \frac{V}{V_0} = \frac{1 + A}{1 + A\exp(F\delta/k_BT)} \quad (8)$$

We also consider the force $F_{1/2}$ at which the velocity drops to half-maximal in Eq. 1

$$F_{1/2} = \frac{k_BT}{\delta}\ln\left(\frac{1 + 2A}{A}\right) \approx \frac{k_BT}{\delta}\ln(a) \quad (9)$$

where $a = A^{-1}$ and the approximation holds because $A < 10^{-4}$ for our data. We define the dimensionless force $f$ as

$$f = F/F_{1/2} = \frac{F\delta}{k_BT\ln(a)} \quad (10)$$

and recast Eq. 1 in terms of the new variables as

$$v(f) = \frac{1 + A}{1 + A\exp(-f\ln A)} \approx \frac{1}{1 + a^{f-1}} \quad (11)$$

where $a$ is the single free parameter remaining in this $f$-$v$ relation. Using this normalization scheme, one can rescale and average experimental data from a heterogeneous ensemble of RNAP complexes and test the fit. Given the general nature of Eq. 11, it may prove applicable to a variety of mechanoenzymes.

### References and Notes

1. M. J. Chamberlin, *Harvey Lect.* **88**, 1 (1994); S. Uptain, C. Kane, M. Chamberlin, *Annu. Rev. Biochem.* **66**, 117 (1997); R. Mooney, I. Artsimovitch, R. Landick, *J. Bacteriol.* **180**, 3265 (1998).
2. H. Yin et al., *Science* **270**, 1653 (1995).
3. D. A. Schafer, J. Gelles, M. P. Sheetz, R. Landick, *Nature* **352**, 444 (1991); H. Yin, R. Landick, J. Gelles, *Biophys. J.* **67**, 2468 (1994).
4. H. Kabata et al., *Science* **262**, 1561 (1993); S. Kasas et al., *Biochemistry* **36**, 461 (1997).
5. R. Landick, *Cell* **88**, 741 (1997); J. Gelles and R. Landick, *ibid.* **93**, 13 (1998).
6. A. V. Hill, *Proc. R. Soc. London Ser. B* **126**, 136 (1938).
7. K. Svoboda and S. M. Block, *Cell* **77**, 773 (1994); A. J. Hunt, F. Gittes, J. Howard, *Biophys. J.* **67**, 766 (1994); C. M. Coppin, D. W. Pierce, L. Hsu, R. D. Vale, *Proc. Natl. Acad. Sci. U.S.A.* **94**, 8539 (1997); H. Kojima, E. Muto, H. Higuchi, T. Yanagida, *Biophys. J.* **73**, 2012 (1997).
8. H. C. Berg and L. Turner, *Biophys. J.* **65**, 2201 (1993).
9. M. D. Wang, Y. Yin, R. Landick, J. Gelles, S. M. Block, *ibid.* **72**, 1335 (1996).
10. Transcription complexes were prepared as described previously and attached to 0.5-$\mu$m-diameter polystyrene beads (2, 3). Voltage signals corresponding to displacement in the interferometer and laser light intensity were low-pass filtered at 1 kHz, digitally sampled by computer at 2 kHz, then averaged and binned at 20 Hz for offline analysis. The interferometer was calibrated and signals were corrected as previously described (9). The corrections adjust for the changes in interferometer sensitivity as beads move vertically away from the trap center and for the geometry as the angle of the DNA changes with respect to the plane of the coverglass during shortening of the tether.
11. Complexes with initial tether lengths >500 nm moving at unloaded speeds >3 nt/s and that reached the clamp limit were selected for analysis. With the clamp active, a stall was operationally defined as beginning at the point where the velocity dropped below ~1.5 nucleotides per second (the experimental drift limit) for more than 10 s. To minimize any sticking of DNA tethers to the coverglass surface, these experiments were conducted in flow chambers treated with blocking proteins, as described (2, 3, 9).
12. We reported previously an RNAP stall force of at least 14 pN. Several lines of evidence suggested that this number may underestimate the actual value (2). First, about 20% of beads drawn by RNAP complexes were not stopped at the fixed laser powers used and escaped from the trap, permitting only a lower bound of 15 to 20 pN to be placed on their stall force. Second, long-term exposure to high levels of laser light damaged a significant proportion of complexes, leading to irreversible stalls (that is, movement that did not recover when the laser power was subsequently reduced). Third, many stalls happened abruptly, as the force increased beyond some threshold, whereas a minority of stalls took place more gradually [see figure 2C of (2)]. This suggested that the stall force might be a function of the particular nucleotide sequence being transcribed. Because force mounted slowly as RNAP traversed comparatively long segments of DNA (typically ~500 base pairs or more), an abrupt stall might correspond to the enzyme reaching a point on the template with a lower intrinsic stall force than its previous positions. Assuming this interpretation to be correct, stall force data acquired for slowly developing loads (at low trap stiffness) would tend to produce biased estimates, preferentially sampling lower values. The feedback system developed here was designed to circumvent these difficulties (Fig. 1D). Once a moving bead reaches a displacement corresponding to some preset limit, the intensity of the laser light is actively servo-controlled (by means of an acousto-optic modulator) to prevent further motion. This clamps the bead at the limit (9), an arrangement that affords several advantages. First, photodamage is minimized; the trap light intensity is kept as low as possible until it becomes necessary to increase it, reducing the overall exposure of RNAP to the laser light by an estimated factor of five relative to earlier work. Higher peak powers are achieved without subjecting molecules to sustained exposure. As a result, all moving beads are now stalled without escaping from the trap. Second, the dynamic response of the system is dramatically improved. Force can be recorded with millisecond resolution (2, 9), and RNAP can be halted within a matter of seconds, 5- to 40-fold faster. Because the DNA tether can be readily pretensioned by the optical trap, the elastic compliance is decreased. With a taut, ~3-kbp DNA tether, bead equilibrium position can be determined with a precision of ~2 nm, corresponding to ~6 base pairs, with 50 ms time resolution (or better). Third, the rapid response of the feedback system stalls the enzyme before it travels as far, leading to a less biased sampling of stall force along the template.
13. Records of bead position were converted to DNA contour length by a variation of the method described (9), taking advantage of the fact that many transcription complexes stopped permanently on the DNA template at the end of experimental runs. Complexes with final tether lengths >300 nm were selected for analysis. With the bead held in the trap, the microscope stage was moved in a preprogrammed fashion, and both the length and elastic properties of the residual tether were measured directly. Using both the final tether length and the force-extension relationship for the DNA molecule, in combination with time records for bead displacement and trap stiffness from the earlier experimental run, the motion of RNAP along the DNA template required to produce such records could be computed. Computed displacements were converted directly to transcript size by assuming that no slippage occurred and that one base pair corresponds to 0.338 nm [W. Saenger, *Principles of Nucleic Acid Structure* (Springer-Verlag, New York, 1988)].
14. R. R. Reisbig and J. E. Hearst, *Biochemistry* **20**, 1907 (1981); K. M. Arndt and M. J. Chamberlin, *J. Mol. Biol.* **213**, 79 (1990); C. L. Chan and R. Landick, in *Transcription: Mechanisms and Regulation*, R. C. Conaway and J. W. Conaway, Eds. (Raven Press, New York, 1994), vol. 3, pp. 297–321.
15. Pauses were removed by applying a threshold template to the velocity data, $V(t)$, and deleting those intervals during which average speed (computed as described) fell below 50% of the template value at any given time. The remaining portions of the record were then concatenated to form a new record. The threshold template function was fixed in advance for each run and consisted of two sequential linear segments: one constant, the next tapering linearly from this constant value to zero at some fixed point in the record. The amplitude of the constant, the slope of the linear taper, and the fixed intercept point were chosen empirically. Taken together, the two line segments roughly approximate the shape of $V(t)$ curves. In principle, it is impossible to distinguish between transient transcriptional pausing and mechanical stalling in the limit that complexes are halted by an external load, based solely on velocity data. Furthermore, uncertainties due to noise and drift make it difficult to ascertain exactly when stall is achieved (11). For these reasons, the shapes of $F$-$V$ curves are poorly determined near their $x$-intercepts (zero velocity).
16. The calculated efficiencies neglect energetic contributions from RNA folding.
17. S. M. Block, *Trends Cell Biol.* **5**, 169 (1995).
18. Transcriptional velocity was computed from compliance-corrected displacement records using a Savitsky-Golay smoothing filter [W. H. Press, S. A. Teukolsky, W. T. Vetterling, B. P. Flannery, *Numerical Recipes in C* (Cambridge Univ. Press, Cambridge, 1992), pp. 650–655]. The window width was chosen by dividing 460 nt/s by the zero-load speed $V_0$, in nt/s.
19. The large heterogeneity in stall force may reflect several contributions. (i) Complexes were oriented randomly on the surface with respect to the direction of the applied load, and the dependence upon angle may be significant; (ii) Stall forces may depend on the template sequence; (iii) Heterogeneity may exist in the properties of nominally identical RNAP molecules.
20. In principle, elongation by RNAP can be arrested by any of a variety of physical mechanisms. (i) The applied load could reversibly halt progress, via mechanochemical coupling in the enzyme; (ii) the load could place the enzyme in a transcriptional pause state; (iii) the load could temporarily inhibit the enzyme, placing it in a state that is biochemically distinct from a pause; or (iv) the enzyme could become irreversibly damaged, either directly by the applied load or by exposure to the laser light. In these and earlier experiments (2), both reversible and irreversible stalls were found, and reversible stalls required the same average force within error as irreversible stalls, suggesting that most damage occurred subsequent to stall. Distinguishing among mechanisms (i) through (iii) is nontrivial and will require additional biochemical, as well as mechanical, data.
21. D. A. Erie, O. Hajiseyedjavadi, M. C. Young, P. H. von Hippel, *Science* **262**, 867 (1993); H. Matsuzaki, G. A.

Kassavetis, E. P. Geiduschek, *J. Mol. Biol.* **235**, 1173 (1994); C. Chan, D. Wang, R. Landick, *ibid.* **268**, 54 (1997).
22. N. Komissarova and M. Kashlev, *J. Biol. Chem.* **272**, 15329 (1997); E. Nudler, A. Mustaev, E. Lukhtanov, A. Goldfarb, *Cell* **89**, 33 (1997).
23. M. Palangat, T. Meier, R. Keene, R. Landick, *Mol. Cell* **1**, 1033 (1998).
24. More complex models for movement can be entertained, including those where the tight-coupling assumption is violated. Such loosely coupled enzymatic schemes are not parsimonious, however, as they involve greater numbers of free parameters.
25. H. Y. Wang, T. Elston, A. Mogilner, G. Oster, *Biophys. J.* **74**, 1186 (1998).
26. F. Jülicher and R. Bruinsma, *ibid.*, p. 1169.
27. M. D. Wang, H. Yin, R. Landick, J. Gelles, S. M. Block, *ibid.* **70**, A44 (1996).
28. K. A. Johnson, *Annu. Rev. Biochem.* **62**, 685 (1993).
29. In these assays as before (*2, 3, 9*), molecules of RNAP were affixed nonspecifically to the coverglass surface. As a result, the applied load, acting through the DNA, is exerted at a random (and unknown) azimuthal angle with respect to the enzyme. Assuming that only some fractional component, $F_{eff}$, of the full load applied at the distal end of the tether, $F$, is effective in slowing transcription, it follows that the apparent $\delta$ (as determined by fits to Eq. 1) will be reduced by the ratio $F_{eff}/F$. Normalization through Eq. 10 permits $F$-$V$ curves with different apparent $\delta$ to be compared, yielding an average value.
30. Supported by grants from the National Institute of General Medical Sciences (R.L., J.G., and S.M.B), and from NSF and the W. M. Keck Foundation (S.M.B). M.D.W. was supported by a Damon Runyon-Walter Winchell Cancer Research fund postdoctoral fellowship. M.J.S. was supported by an American Heart Association predoctoral fellowship and a Proctor Honorific Fellowship from Princeton University. S.M.B. and M.D.W. thank S. Gross, L. Satterwhite, and K. Visscher for helpful discussions and advice, and K. Neuman for comments on an early draft of the manuscript. A movie of the tether-particle assay can be viewed at www.rose.brandeis.edu/users/gelles/stall/